Journal of
Applied Research in Water and Wastewater
Journal homepage: www.arww.razi.ac.ir

Original paper

Kinetics of photocatalytic degradation of reactive black B using core-shell TiO_2-coated magnetic nanoparticle, $Fe_3O_4@SiO_2@TiO_2$

Saeed Aghel, Nader Bahramifar*, Habibollah Younesi

Department of Environmental pollution, Faculty of Natural Resources & Marine Science, Tarbiat Modares University, Tehran, Iran.

ARTICLE INFO

Article history:
Received 28 July 2016
Received in revised form 8 September 2016
Accepted 1 October 2016

Keywords:
Photocatalytic Degradation
kinetics
Reactive Black B
magnetic nanoparticle

ABSTRACT

In particular, the inappropriate/inevitably discharge of dye-containing effluents is undesirable because of their color, resistant to the biological treatment systems, toxic, and their carcinogenic or mutagenic nature to life forms. About fifty percent of the washing dye liquor is discharged into the water environment. $Fe_3O_4@SiO_2@TiO_2$ nanoparticles, were prepared, characterized and tested as photocatalyst in the removal of Reactive Black B (RBB) dye by a photocatalytic process. The effect of photocatalyst concentration, pH and temperature in the photodegradation kinetics is discussed in terms of the Langmuir–Hinshelwood (L-H) model. SEM and TEM characterizations confirmed the $Fe_3O_4@SiO_2@TiO_2$ nanoparticel, revealed that the obtained particles a spherical morphology with sizes about 100 nm. The DRS pattern of $Fe_3O_4@SiO_2@TiO_2$ shows the energy band gap value of photocatalyst is 2.75 eV. The presence of Fe_3O_4, SiO_2 and anatase TiO_2 in the as-synthesis magnetic nanoparticle were confirmed by FTIR and XRD analysis. The $Fe_3O_4@SiO_2@TiO_2$ photocatalyst in combination with ultraviolet irradiation and under optimal conditions can destroy 100% of RBB after 120 min. Furthermore, the magnetic photocatalyst was efficiently separated from the solution with the help of a magnet and shown the capable of reusability up to 10 times without reducing their efficiency.

1. Introduction

Textile industries widely use complex synthetic organic colorants as coloring agents which produce colored wastewater, since the dye is not absolutely adsorbed by the textile. The release of this wastewater to the environment is Dangerous to aquatic life (King-Thom. 1993) and mutagenic to humans (Lucas and Peres. 2006). These textile wastewater, usually with dye contents about 10–200 mg/L (F.P. van der Zee. 2002) create a bulky problem to wastewater treatment plants in the whole world. The customary treatment methods usually applied to textile wastewaters, such as flocculation/coagulation, adsorption on the surface of activated carbon or membrane separation, only lead to the phase transference of the contaminant from liquid phase to the solid phase (Lucas et al. 2007). Biological treatments are also not a good solution because of the biological resistance of most pigment. Therefore, the removal of these dyes before release into the environment is a precedence. Advanced oxidation processes (AOPs) arose as a suitable method for the degradation of organic pollutants in wastewater (Litter. 1999).

AOPs inclusive Fenton reaction, Ozonation, photolysis, wet air oxidation, ultrasounds and photocatalysts. Photocatalysts are a wide application in the total degradation of organic pollutants into CO_2 and H_2O (Xu. 2007; Beydoun et al. 2000) Among all semiconductor photocatalysts, TiO_2 is the widely applied as photocatalyst because it is non-toxic, chemically stable, inexpensive and its photogenerated electrons and holes are highly reducing and oxidizing, respectively (Litter. 1999). A Usual method to separation the catalyst in slurry-type reactors is by sedimentation of TiO_2 particles after pH adjustment followed by a flocculation–coagulation process; however, these processes are expensive in terms of time, manpower and reagents. One Technique to overcome the separation problem is through the making of titanium dioxide with magnetic properties, Magnetic separation constitutes a more sustainable process since it prevents catalyst mass losses and the use of additional solvents. It has been established that the direct contact between the TiO_2 shell and the iron oxide magnetic cores may lead to low photoactivity because Fe_3O_4 act as recombination centers for electrons and positive holes, especially in the case of Fe_3O_4 (Beydoun et al. 2000) The use of a buffer SiO_2 layer between the magnetic core and the TiO_2 shell, i.e. $Fe_3O_4@SiO_2@TiO_2$, improves the photocatalytic activity of the nanomaterial by preventing the injection of charges from TiO_2 shell to the magnetic cores (Chen et al. 2001) In this study, the kinetic and equilibrium data were modeled using Langmuir–Hinshelwood (L–H) model.

2. Materials and methods

2.1. Materials and reagents

Hydrochloric acid (HCl), Iron (III) chloride hexahydrate, sodium acetate anhydrous (NaAc), tetrabutyl orto titanate (TBOT, 97 %), n-hexane, ethylene glycol, Ethylene Diamine Tetra Acetic acid disodium salt (EDTA-2Na) and sodium silicate were purchased from Merck Company. during all steps when water was needed, deionized water was used throughout.

2.2. Synthesis of Fe_3O_4

Fe_3O_4 magnetic Nano particles were synthesized according to the method reported by Lin et al. 2013. first (2.5 mmol, 0.68 g) $FeCl_3{\cdot}6H_2O$, and (0.015 mol, 1.2 g) NaAc were dissolved in (20 ml) ethylene glycol under magnetic stirring until the solution became clear, then (0.01 mmol, 0.034 g) EDTA-2Na was add to this solution and sonicate at 37 Hz for 30 min, the resulting was transferred to a Teflon-lined stainless-steel autoclave. The autoclave was sealed and heated at 180 −200 °C for 8−10 h and naturally cooled to room temperature. After that, the black particles were washed with deionized water and ethanol three times and then dried under vacuum at 50 °C (Lin et al. 2013).

2.3. Synthesis of $Fe_3O_4@SiO_2$

*Corresponding author Email: n.bahramifar@modares.ac.ir

Please cite this article as: S. Aghel, N. Bahramifar, H. Younesi Kinetics of Photocatalytic Degradation of Reactive Black B Using Core-shell TiO_2-Coated Magnetic Nanoparticle, $Fe_3O_4@SiO_2@TiO_2$, Journal of Applied Research in Water and Wastewater, 3 (2), 2016, 253-259.

For Synthesis of Fe_3O_4@SiO_2 Briefly 1.3 g of sodium silicate was dissolved in 100 ml deionized water (which was heated to 80 °C) under magnetic stirring to form a clear solution. then 0.3 g of Fe_3O_4 put into the solution. The pH value of the mixture was adjusted to 6.5 with 2 mol/L HCl solution. The mixture was further stirred at 80 °C for 180 min. The resulting silica-coated Fe_3O_4 nanoparticles were collected with the help of a magnet and washed with deionized water and, followed by drying in Freeze Dryer for 24 h (Wang et al. 2010).

2.4. Synthesis of Fe_3O_4@SiO_2@TiO_2

The preparation procedure of Fe_3O_4@SiO_2@TiO_2 described by Lirong et al. 2014. Briefly 0.2 g as-prepared Fe_3O_4@SiO_2 particles were dispersed in a mixture of hexane (70 ml) and deionized water (0.2 ml), followed by the addition of TBOT (0.5ml) under ultrasonication treatment at 50 Hz for 90 min. The mixture was transferred to Teflon-lined autoclave. It was heated at 100 °C for 180 min. The precipitates were collected by magnet and washed with hexane three times, then dried at room temperature. the obtained Fe_3O_4@SiO_2@TiO_2 particles were calcined at 500 °C for 180 min (Lirong et al. 2014).

2.5. Synthesis of Fe_3O_4@SiO_2@TiO_2

For assessment of the photocatalytic activity of the Fe_3O_4@SiO_2@TiO_2 nanoparticel, we used a solution of RBB. The photocatalytic experiments were done in beaker 400ml including 100 ml of 50 mg/L dye solution. For unlimbering favorite Ultraviolet photon, we implemented UV lamps of 8 W (Philips, Holland) in Quartz chamber in beaker Content of 50 mg/L RBB. In order to make the solution homogenous used the magnetic stirrer during the irradiation. At the beginning of each experiment, we turned off the UV lamps for 15 minutes and then we turned them on. Samples of the solution were obtained after, 15, 30, 45,60,75,90,105,120 min.

2.6. Parameter effects on the removal of RBB

The effects of the Fe_3O_4@SiO_2@TiO_2 dose (50, 100, 150 and 200 mg/l) on the removal of RBB were Examined. In the photocatalytic process, pH is one of the most important operating parameters that affect the charge on the catalyst. The effect of different initial pH on the dye removal was investigated by mixing 150 mg of Fe_3O_4@SiO_2@TiO_2 photocatalyst dose at 25 °C for 120 min. The pH was adjusted to values 3-9 (from acidic to basic) using 1 M HCl and 1 M NaOH solution.

2.7. Kinetics of photocatalytic degradation of RBB

For investigation photodegradation reaction, we use the Langmuir–Hinshelwood model to description the initial rates of photodegradation of dye.

$$r_0 = \frac{-dC}{dt} = \frac{krKC}{1+KC} \quad k_rKC = k_{app}C \tag{1}$$

where r_0 is the initial rate of the removal of the RBB. t the reaction time and *C*, the equilibrium bulk-solute dose. K indicant the equilibrium constant for absorption of dye on the surface of photocatalyst and kr represent the limiting rate constant of the reaction at maximum coverage under the given experimental conditions. In the case of highly diluted solution and the term KC becomes less than 1, when the denominator of Eq. (1) neglected and the rate data can be modeled by the apparent first-order kinetics as in the following equation:

$$r = \frac{-dC}{dt} = krKC = k_{app}C \tag{2}$$

where C is the dye concentration at time t, and kapp the apparent first-order rate constant. Integrating Eq. (2) And using boundary condition $C= C_0$ at t = 0 gives:

$$\ln\left(\frac{c_t}{c_0}\right) = -k_{app}t \tag{3}$$

where C_0 is the dye concentration at the initial time.

2.8. Physico-chemical characterization

X-ray diffraction (XRD) of the products were obtained on Philips Xpert MPD diffractometer. The morphology and microstructure of products were characterized by scanning electron microscopy (SEM, LEO,1455VP, Cambridge, U.K) and CM120 transmission electron microscopy (TEM). Fourier Transform Infrared (FT-IR) spectra were recorded on (Shimadzo, FT_IR1650 spectrophotometer, Japan) using KBr pellets for samples. The magnetic properties of the photocatalyst were quantified using a Vibrating Sample Magnetometer (VSM) at a temperature range of 1.8 to 310 K with a Meghnatis Daghigh Kavir Co. UV-Vis absorption spectra of products were recorded by a Diffuse Reflectance Spectroscopy (DRS) V/650 spectrophotometer (Jasco Inc., Japan) with a wavelength range from 220 to 1020 nm. XRD patterns of Fe_3O_4, Fe_3O_4@SiO_2 and Fe_3O_4@SiO_2@TiO_2 are shown in Fig1. As shown, in general, all the powders are well-crystalline materials. For Fe_3O_4 core, seven diffraction peaks were observed in 2θ =18.5, 30.5, 35.5, 43.2, 53.5, 57.1 and 62.6 (Fig. 1a). This pattern is corresponding to crystalline Fe_3O_4 magnetic nanostructures. (Wang et al. 2012) The XRD pattern of the Fe_3O_4@SiO_2 sample shows almost the same feature as pure Fe_3O_4, except that a broad peak centered at 15-25 of 2θ corresponding to SiO_2 was observed, indicating that the prepared SiO_2 is amorphous (Jian et al. 2012) (Fig. 1b). In the XRD results for Fe_3O_4@SiO_2@TiO_2 some peaks were emerged that is related to TiO_2 semiconductor. The emerged peak at 2θ = 25.37, 38.11, 48.07, 54.14 is shown the anatase phase for TiO_2 (Jian et al. 2012) (Fig. 1C). In addition, no other peak is observed belonging to any adsorbed impurities or phase in the sample structure. Moreover, the sharp diffraction peaks show that the obtained nanoparticles have high crystallinity.

FT-IR measurements were performed for Fe_3O_4, Fe_3O_4@SiO_2 and Fe_3O_4@SiO_2@TiO_2 samples as shown in Fig. 2 all spectra present absorption peak at 578 cm^{-1}, corresponding to the Fe–O vibration from the magnetite phase (Yamaura et al. 2004). Spectrum of Fe_3O_4@SiO_2 present the typical Si-O-Si bands of the inorganic symmetric vibration modes around 786 cm^{-1}, asymmetric stretching vibration around 1033 – 1100 cm^{-1} and the band at 964 cm^{-1} is assigned to the Si-O stretch that indicates the silica layer around the Fe_3O_4 (Innocenzi. 2003; Pillay et al. 2013). The Fe_3O_4@SiO_2@TiO_2 spectra are shown in Fig. 2C. The peak at 500-850 cm^{-1}, which corresponds to the Ti-O band and new absorption band covering a range from 859 to 1087 cm-1, which corresponds to the stretching vibration of Ti-O-Si, was appeared in the FT-IR spectra of Fe_3O_4@SiO_2@TiO_2 as compared to Fe_3O_4@SiO_2 (Ghasemi et al. 2016).

Therefore, the photocatalyst is not a simple mechanical mixture of TiO_2 anatase and Fe_3O_4@SiO_2 but it is a nanocomposite regarding the formation of mentioned new bonds. The morphologies of Fe_3O_4@SiO_2@TiO_2 powder were studied by scanning electron microscopy illustrated in Fig 3. In SEM, a focused electron beam scans conductive sample surface reveals information about the sample including external morphology (texture) and topography. This analysis reveals that for Fe_3O_4 synthesized by Solvothermal method, particles almost are nano-size with mediocre size about 80-90 nm (Fig. 3A). When the surface of Fe_3O_4@SiO_2 particles was coated with layers of TiO_2 via sol–gel procedures, the roughness and the size of particles have been increased to mediocre size about 100 nm for Fe_3O_4@SiO_2@TiO_2 nanostructures (Fig. 3B).

Please cite this article as: S. Aghel, N. Bahramifar, H. Younesi Kinetics of Photocatalytic Degradation of Reactive Black B Using Core-shell TiO_2-Coated Magnetic Nanoparticle, Fe_3O_4@SiO_2@TiO_2, Journal of Applied Research in Water and Wastewater, 3 (2), 2016, 253-259.

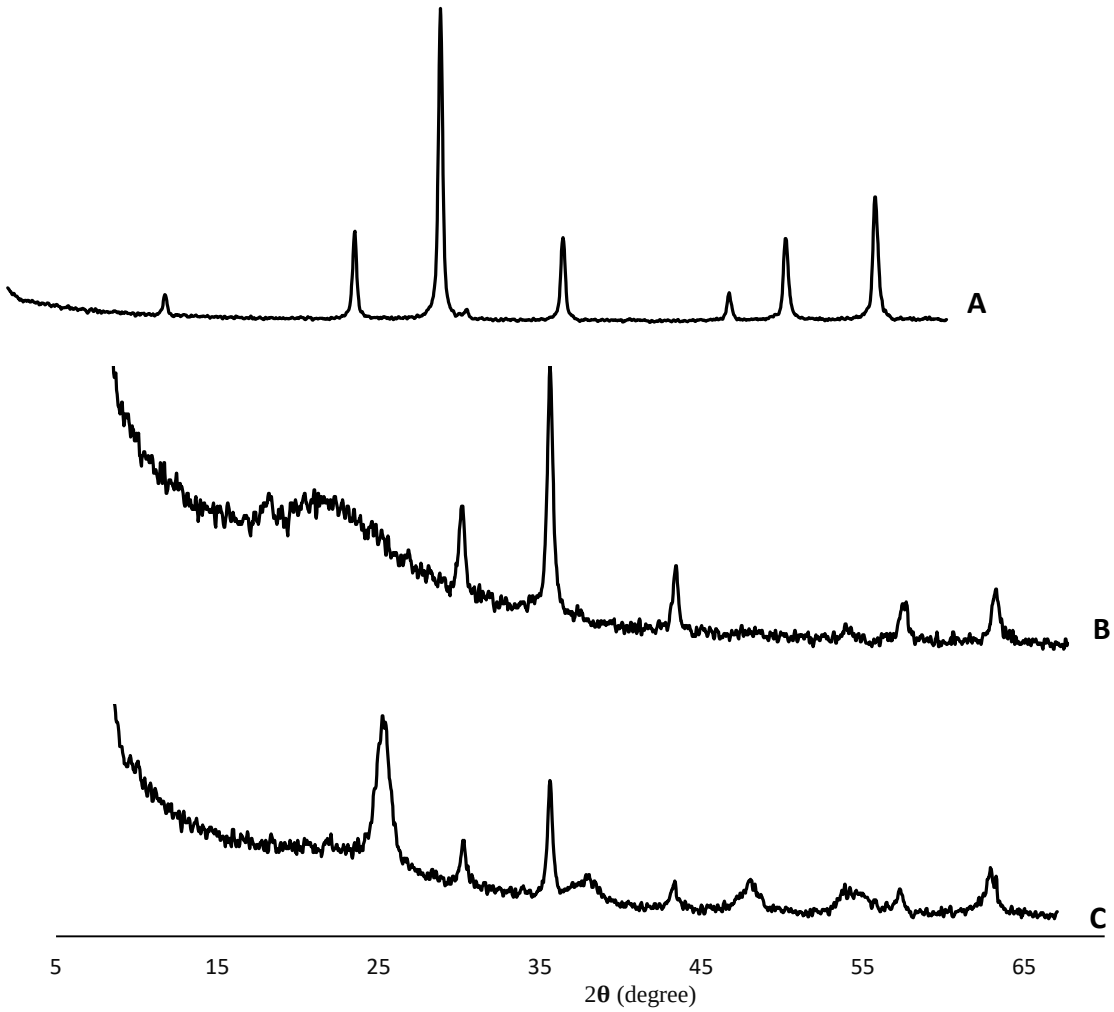

Fig 1. XRD pattern of Fe_3O_4 (A), $Fe_3O_4@SiO_2$ (B) and $Fe_3O_4@SiO_2@TiO_2$ composites (C).

The TEM images of the $Fe_3O_4@SiO_2@TiO_2$ nanoparticles are shown in Fig. 4, The core-shell structure can be clearly distinguished because of the different color contrast between the cores and shells. It can be seen that the shape of nanoparticles is almost spherical with an average diameter of 100 nm.

For studying magnetization treatment of the as-prepared nanoparticles, the magnetization curve of Fe_3O_4, silica coated Fe_3O_4 and $Fe_3O_4@SiO_2@TiO_2$ samples was measured at room temperature, as shown in Fig3. Results indicate that the magnetic hysteresis loops are S-like curves. Also, the magnetic remanence of the all samples was nearly zero, suggesting that samples exhibit a superparamagnetic behavior. The specific saturation magnetizations (*M*s) are 76, 23 and 12 emu/mg for Fe_3O_4, $Fe_3O_4@SiO_2$ and $Fe_3O_4@SiO_2@TiO_2$ samples, respectively. The reduction in the value of *M*s could be attributed to the rather smaller size of the Fe_3O_4 nanoparticles and the added mass of some layers which were nonmagnetic on them. Due to this magnetic property, $Fe_3O_4@SiO_2@TiO_2$ could move regularly under the action of an external magnet after they congregated.

The absorption coefficient and optical band gap of a material are two important parameters which controlling a photocatalytic activity and this feature relevant to the electronic structure of the material. It can be seen from the Fig4 that the absorption is around 450 nm for $Fe_3O_4@SiO_2@TiO_2$, this absorption extends into the visible region. The band gap energy value of corresponding spectrum was calculated using the equation $E_{bg} = 1239.8/\lambda$ nm (Velmurugan et al.2011) The band gap energy value of for $Fe_3O_4@SiO_2@TiO_2$ is 2.75 eV.

3. Results and discussion

3.1. Effect of photocatalyst concentration

The effect of $Fe_3O_4@SiO_2@TiO_2$ dosage on the rate of dye removal was Investigated (Fig. 7A). The first-order rate constant Was obtained for photocatalyst dosage of 50, 100, 150 and 200 mg/l (Fig. 7B). The design of $\ln(C_t/C_o)$ against reaction time gives a good linear relevance (with $R^2 > 0.96$), which is witness of the good agreement of fitting the reaction data in first-order reaction. According the dosage of the $Fe_3O_4@SiO_2@TiO_2$ and their rate constants in the dye removal reaction (Fig. 7B), it can be said the concentration of the $Fe_3O_4@SiO_2@TiO_2$ Positive correlation with photocatalytic operation, it shows that removal of RBB is dependent on the number of available electron hole pair. The photocatalytic removal of dye in numerous cases Revealed this behavior (Chen and Liu. 2007). The maximum photocatalytic degradation efficiency was obtained at a photocatalyst dosage of 200 mg/l. It has been found that the rate of photocatalytic degradation increases with increasing for photocatalyst dosage from 50 to 200 mg/l; it is clear that k_{app} increased with an increase in $Fe_3O_4@SiO_2@TiO_2$ dosage.

Please cite this article as: S. Aghel, N. Bahramifar, H. Younesi Kinetics of Photocatalytic Degradation of Reactive Black B Using Core-shell TiO_2-Coated Magnetic Nanoparticle, $Fe_3O_4@SiO_2@TiO_2$, Journal of Applied Research in Water and Wastewater, 3 (2), 2016, 253-259.

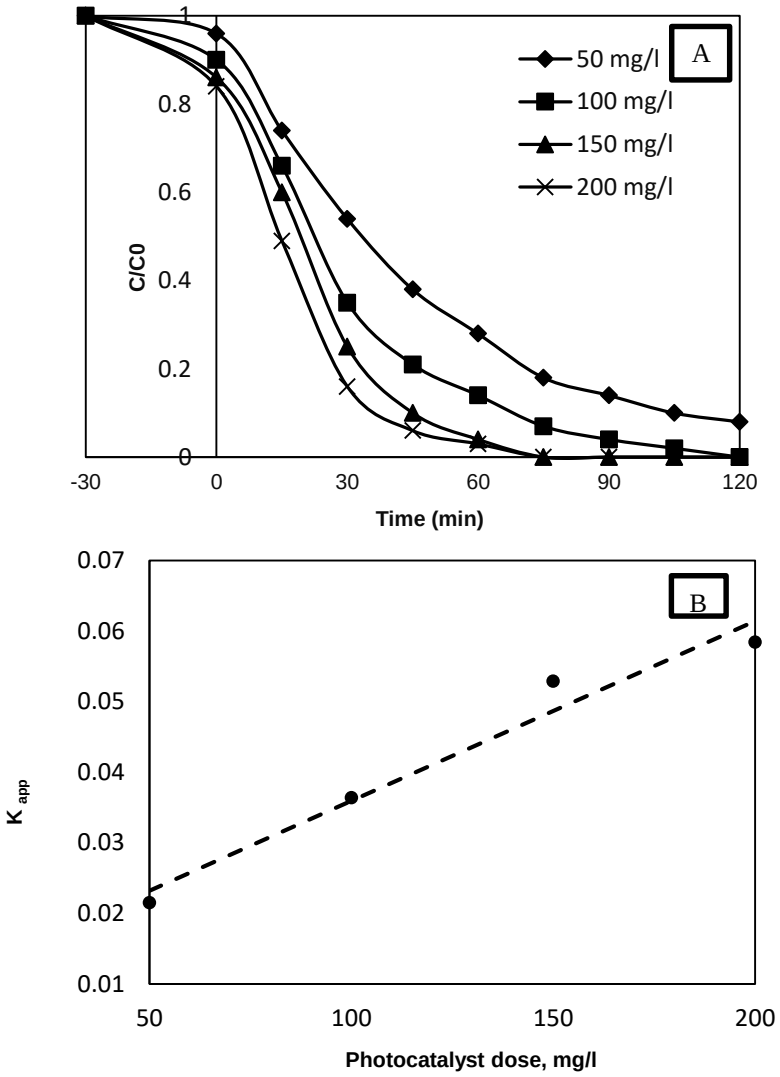

Fig 7. Effect of photocatalyst concentration on dye removal rate (A) and effect of different amounts of photocatalyst concentration on the kinetic rate constant (B).

3.2. Effect of pH

The pH value of the Solution is an essential operational factor on the surface charge properties of the TiO_2, the absorption behavior of dye and removal of dye taking place on the surface of $Fe_3O_4@SiO_2@TiO_2$ Nanoparticle (Khodadoust et al. 2012). Therefore, it is important to study the role of pH on Photocatalytic process and specify the optimal pH for dye removal (Diya'uddeen et al. 2011). Fig. 8A shows the efficiency of $Fe_3O_4@SiO_2@TiO_2$ Nanoparticle for dye removal as a function of pH under using 150 mg/l photocatalyst dosage at a temperature of 25 °C for 120 min. The apparent first-order rate constant for the reaction of $Fe_3O_4@SiO_2@TiO_2$ with dye decreased linearly with pH increasing (Fig. 8B). The maximum efficiency of removal of RBB 100 % was observed at pH 3. The influence of pH on the photocatalytic processes can be described on the basis of the point of zero charge (PZC) of TiO_2 and the absorption of the Organic materials on the TiO_2 in different pH values (Evgenidou et al. 2005). According to the PZC of TiO_2 catalyst, its surface charge is positive in acidic solution and negative in basic solution, respectively (Malato et al. 2009). The RBB is an anionic species of dye, the adsorption of RBB on the surface of TiO_2 is better in acidic pH (Lucas et al. 2013).

3.3. Effect of temperature

The effect of temperature on the dye removal rate was significant (Fig. 9A). The results showed that the dye removal rate Decrease as the temperature rose. The photocatalytic activity of $Fe_3O_4@SiO_2@TiO_2$ was tested at 150 mg/l photocatalyst concentration and pH under varying temperatures from 15 to 65 °C. The maximum removal efficiency was achieved at a temperature of 15 °C. The apparent first-order rate constant for the reaction of $Fe_3O_4@SiO_2@TiO_2$ with dye Decrease linearly with increasing temperature (Fig. 9B), which further confirms that the dye removal is not an Endothermic reaction.

3.4. Studies upon photocatalyst recycling

The Durability and Reusability of the magnetic nanoparticle upon several times is a key issue, since one of the basic Bugs of non-magnetic photocatalyst process is the catalyst separating and reuse. The Greatest advantage of the magnetic photocatalyst is the easily separation after the photocatalytic Process. The $Fe_3O_4@SiO_2@TiO_2$ was separated and reused in further 10 times. Fig. 10 summarizes the efficiency of dye removal (in percentage).

Please cite this article as: S. Aghel, N. Bahramifar, H. Younesi Kinetics of Photocatalytic Degradation of Reactive Black B Using Core-shell TiO_2-Coated Magnetic Nanoparticle, $Fe_3O_4@SiO_2@TiO_2$, Journal of Applied Research in Water and Wastewater, 3 (2), 2016, 253-259.

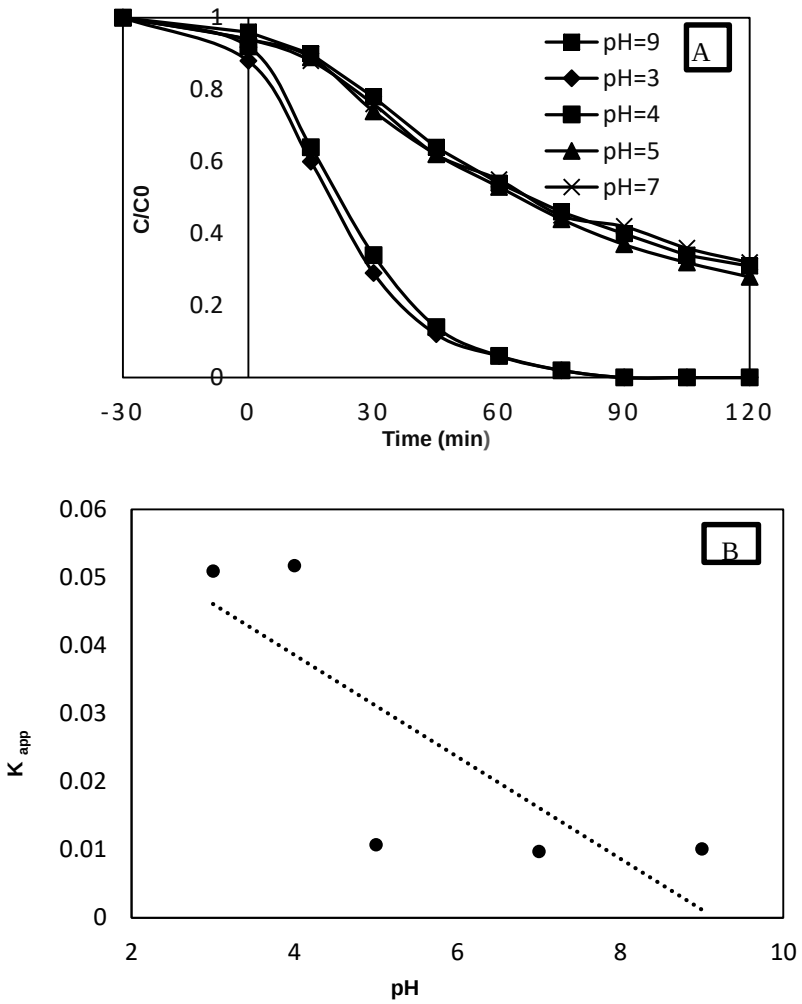

Fig 8. Effect of pH on dye removal rate(A) and photocatalytic rate constant as a function of pH(B).

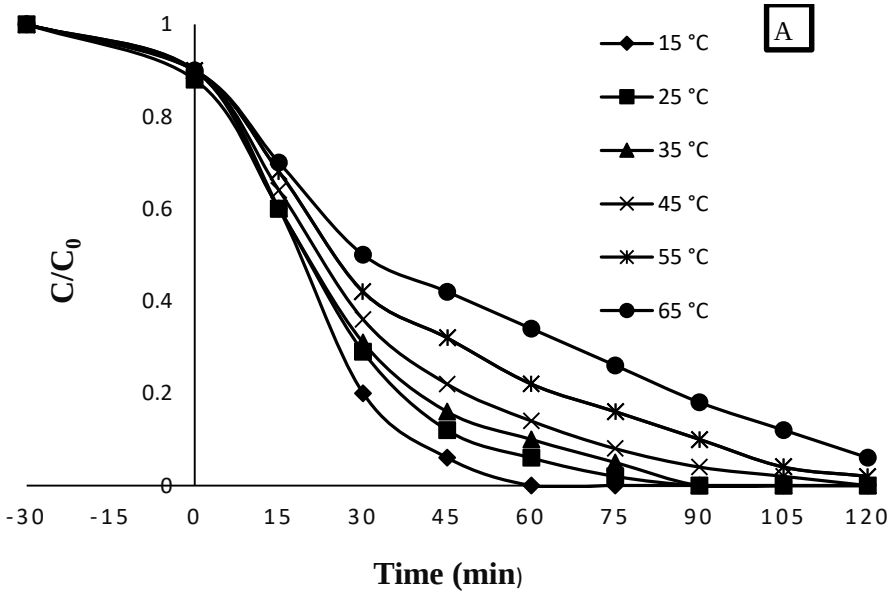

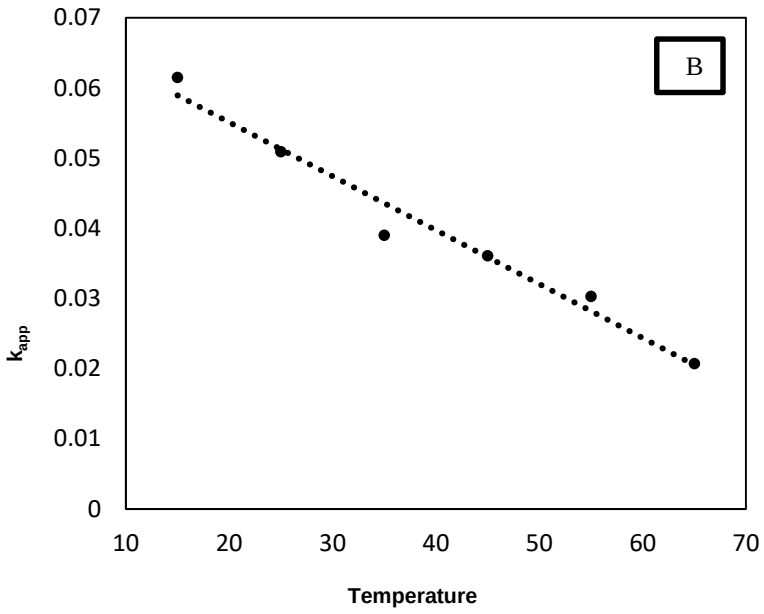

Fig 9. (A) Effect of temperature on dye removal rate and (B) photocatalytic rate constant as a function of temperature.

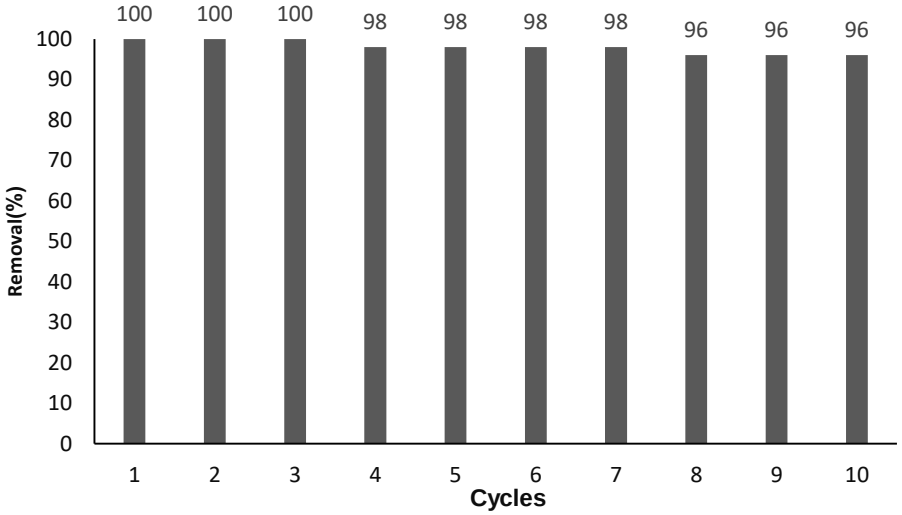

Fig 10. Reusability of photocatalyst for dye removal.

4. Conclusions

A magnetic nanoparticel $Fe_3O_4@SiO_2@TiO_2$ was successfully synthesized and tested in the RBB removal. The fabricated materials were used in the photodegradation of RBB under UV light irradiation, and it was shown that nanospheres had high photodegradation efficiency. In addition, the current study reveals that the fabricated nanospheres displayed good magnetic properties at room temperature, which can create a fast separation photocatalyst after reaction. The results indicate that after ten cycles of use, the high photocatalytic activity of the $Fe_3O_4@SiO_2@TiO_2$ nanocatalyst did not decrease. Therefore, the nanocatalyst are promising agents and highly beneficial for various potential applications for the treatment of textile effluents containing harmful organic dyes. The dye removal rate increased with the increasing of $Fe_3O_4@SiO_2@TiO_2$ dosage to 200 mg/l. pH value of 3 was determined to be Optimize for dye removal and removal rate was much faster at pH less than 4 compared with higher.

References

Beydoun D., Amal R., Low G.K.C., McEvoy S., Novel photocatalyst: titania-coated magnetite. Activity and photodissolution, The Journal of Physical Chemistry B 104 (2000) 4387-4396.

Chen F., Xie Y., Zhao J., Lu G., Photocatalytic degradation of dyes on a magnetically separated photocatalyst under visible and UV irradiation, Chemosphere 44 (2001) 1159-1168.

Please cite this article as: S. Aghel, N. Bahramifar, H. Younesi Kinetics of Photocatalytic Degradation of Reactive Black B Using Core-shell TiO_2-Coated Magnetic Nanoparticle, $Fe_3O_4@SiO_2@TiO_2$, Journal of Applied Research in Water and Wastewater, 3 (2), 2016, 253-259.

Chen S., Liu Y. Study on the photocatalytic degradation of glyphosate by TiO_2 photocatalyst, Chemosphere 67 (2007) 1010-1017.

Evgenidou E., Fytianos K., Poulios I., Photocatalytic oxidation of dimethoate in aqueous solutions, Journal of Photochemistry and Photobiology A: Chemistry 175 (2005) 29-38.

Ghasemi Z., Younesi H., Zinatizadeh A.A., Preparation, characterization and photocatalytic application of TiO_2/Fe-ZSM-5 nanocomposite for the treatment of petroleum refinery wastewater: Optimization of process parameters by response surface methodology, Chemosphere 159 (2016) 552-564.

Innocenzi P., Infrared spectroscopy of sol–gel derived silica-based films: a spectra-microstructure overview, Journal of Non-Crystalline Solids 316 (2003) 309-319.

Jian G., Liu Y., He X., Chen L., Zhang Y., Click chemistry: a new facile and efficient strategy for the preparation of Fe_3O_4 nanoparticles covalently functionalized with IDA-Cu and their application in the depletion of abundant protein in blood samples, Nanoscale 4 (2012) 6336-6342.

Khodadoust S., Sheini A., Armand N. Photocatalytic degradation of monoethanolamine in wastewater using nanosized TiO_2 loaded on clinoptilolite, Spectrochimica Acta Part A: Molecular and Biomolecular Spectroscopy 92 (2012) 91-95.

King-Thom C., Degradation of azo dyes by envi ronmental microorganisms and helminthes, Environmental Toxicology and Chemistry 13 (1993) 2121-2132.

Lin M., Huang H., Liu Z., Liu Y., Ge J., Fang Y., Growth–dissolution–regrowth transitions of Fe_3O_4 nanoparticles as building blocks for 3D magnetic nanoparticle clusters under hydrothermal conditions, Langmuir 29 (2013) 15433-15441.

Lirong M., Jianjun S., Ming Z., Jie H., Synthesis of Magnetic Sonophotocatalyst and its Enhanced Biodegradability of Organophosphate Pesticide, Bulletin of the Korean Chemical Society 35 (2014) 21-35.

Litter M.I., Heterogeneous photocatalysis: transition metal ions in photocatalytic systems. Applied Catalysis B: Environmental, 23 (1999) 89-114.

Lucas M.S., Peres J.A., Decolorization of the azo dye Reactive Black 5 by Fenton and Photo-Fenton oxidation, Dyes and Pigments 71 (2006) 236-244.

Lucas M.S., Dias A.A., Sampaio A., Amaral C., Peres J.A., Degradation of a textile reactive Azo dye by a combined chemical–biological process: Fenton's reagent-yeast, Water research 41 (2007) 1103-1109.

Lucas M.S., Tavares P.B., Peres J.A., Faria J.L., Rocha, M., Pereira C., Freire C., Photocatalytic degradation of Reactive Black 5 with TiO_2-coated magnetic nanoparticles, Catalysis today 209 (2013) 116-121.

Malato S., Fernández-Ibáñez P., Maldonado M.I., Blanco J., Gernjak W., Decontamination and disinfection of water by solar photocatalysis: recent overview and trends, Catalysis Today 147 (2009) 1-59.

Pillay K., Cukrowska E.M., Coville N.J., Improved uptake of mercury by sulphur-containing carbon nanotubes, Microchemical Journal 108 (2013) 124-130.

Velmurugan, R., Sreedhar, B., Swaminathan, M. Nanostructured AgBr loaded TiO_2: an efficient sunlight active photocatalyst for degradation of reactive Red 120. Chemistry Central Journal, 5 (2011). 46.

Wang J., Zheng S., Shao Y., Liu J., Xu Z., Zhu D., Amino-functionalized Fe_3O_4@SiO_2 core–shell magnetic nanomaterial as a novel adsorbent for aqueous heavy metals removal, Journal of Colloid and Interface Science 349 (2010) 293-299.

Wang R., Wang X., Xi X., Hu R., Jiang G., Preparation and photocatalytic activity of magnetic Fe_3O_4/SiO_2/TiO_2 composites, Advances in Materials Science and Engineering (2012) 1-8.

Xu S., Shangguan W., Yuan J., Chen M., Shi J., Preparations and photocatalytic properties of magnetically separable nitrogen-doped TiO_2 supported on nickel ferrite, Applied Catalysis B: Environmental 71 (2007) 177-184.

Yamaura M., Camilo R.L., Sampaio L.C., Macedo M.A., Nakamura M., Toma H.E., Preparation and characterization of (3-aminopropyl) triethoxysilane-coated magnetite nanoparticles, Journal of Magnetism and Magnetic Materials 279 (2004) 210-217.

Zee F.P., Anaerobic azo dye reduction, Ph.D. Thesis, Wageningen University, Wageningen, The Netherlands, (2002), p. 142.

Please cite this article as: S. Aghel, N. Bahramifar, H. Younesi Kinetics of Photocatalytic Degradation of Reactive Black B Using Core-shell TiO_2-Coated Magnetic Nanoparticle, Fe_3O_4@SiO_2@TiO_2, Journal of Applied Research in Water and Wastewater, 3 (2), 2016, 253-259.